

# RADIO-INTERFEROMETER FOR GEOSYNCHRONOUS ORBIT SURVEY

S. Kawase

*NICT Space Communication Center, Kashima, 314-0012 Japan, <http://www.nict.go.jp/ka/control>*

**ABSTRACT:** We developed an interferometer capable of determining satellite positions without ambiguity. It has a 13m-long baseline that rotates in the horizontal plane and tracks Ku/C-band satellite signals. The system enables tracking of any satellite with no prior information, and measures orbital motion to within 0.01 degrees in real time. Examples of measurement demonstrate the potential usefulness of the interferometer for surveying the state of orbital congestion.

## 1. INTRODUCTION

With more and more communication satellites operating in geosynchronous orbits, there is growing concern about possible RF interference between satellites and their potential close proximity. As a result, radio administration authorities in several countries have begun monitoring orbits and frequencies [1]. Monitoring stations usually have large parabolic antennas for radio-spectrum observations and, theoretically speaking, these antennas are able to track satellite motions. In reality, however, tracking antennas tend to include several sources of error, such as structural, thermal-deformation, and driving-mechanism errors, that prevent accurate monitoring of orbits. To overcome this problem, we developed a new monitoring technique.

To support orbit/frequency monitoring, our technique needed to meet the following requirements:

- Use passive reception of satellite signals. Signals may be strong or weak
  - Track communication signals, as beacons may not be known
  - Operate in the most congested frequency bands, Ku (11-12 GHz) and C (3-4 GHz)
  - Estimate orbital motions in latitude and longitude, down to 0.01 degrees or better, preferably in real time
- To meet these requirements, we considered the use of radio interferometry [2]. Interferometry is not a new technique, but because of the following difficulties it is not often used for satellite tracking:

- Measured phases contain ambiguous  $2n\pi$ , with an arbitrary integer  $n$
- Cables connecting antennas cause phase instability as temperatures change

We designed an interferometer that would overcome these difficulties and meet the above requirements. The following sections describe the hardware used for the interferometer, its operation for orbit estimation, and error calibration of the system.

## 2. INTERFEROMETER HARDWARE

A diagram of our interferometer is shown in Fig. 1. A microwave signal from a geosynchronous satellite is reflected by a mirror,  $M_1$ , and then by another mirror,  $M_3$ , before being directed to a fixed antenna,  $A_1$ . The same process occurs at  $M_2$ ,  $M_4$ , and  $A_2$ . Mirrors  $M_1$  and  $M_2$  are mounted on an arm that can rotate to any horizontal orientation. When the arm rotates, the angle of the mirrors is controlled so that the satellite microwaves are directed correctly to the fixed antennas. The mirrors are all planar mirrors with 2-m sides, the fixed antennas are 1.8-m in diameter, and the rotary arm is 13-m long. Mirror-antenna distances ( $M_3$ - $A_1$  and  $M_4$ - $A_2$ ) are 16 m, while mirror-mirror distances ( $M_1$ - $M_3$  and  $M_2$ - $M_4$ ) vary from 15 to 28 m as the arm rotates. These distances are short so that the reflected microwave beams propagate by geometrical optics without refraction.

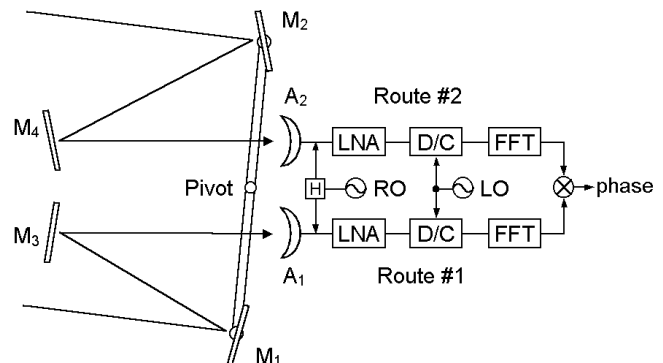


Fig. 1 Interferometer diagram

We measure the phase of the satellite signal between antennas  $A_1$  and  $A_2$ , using an established technique called correlation processing. A common local oscillator (LO) is used to synchronize the phases of the two receiving routes, and a common reference oscillator (RO) is used to compensate for phase-delay variations in receiving routes.

Signal delay along the reflected path  $M_1$ - $M_3$ - $A_1$  and that along  $M_2$ - $M_4$ - $A_2$  is known from the interferometer geometry. If we correct the measured phase for these reflected path delays, we can regard antennas  $A_1$  and  $A_2$  as being mounted on the rotary arm, as illustrated in Fig. 2. Although this “antenna-on-the-arm” system is simple and has several appealing features, in reality, there are some difficulties. Cables must carry RF signals from the

antennas to a phase-measuring unit, and as the arm rotates the twisting cables cause phase errors. Applying antenna weights at the end-points of the arm reduces mechanical precision. With the “mirror-reflecting” design depicted in Fig. 1, antennas  $A_1$  and  $A_2$  are placed side by side, allowing the signals from LO and RO to be distributed via short cables. This is important for preventing phase errors with changes in cable temperatures. For these reasons we selected a mirror-reflecting design for our interferometer.

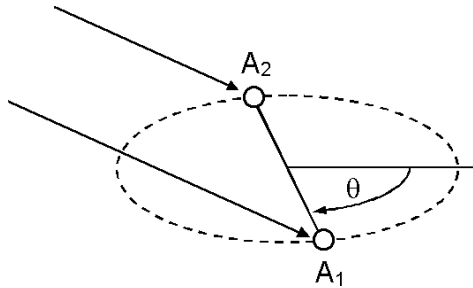


Fig. 2 Antenna-on-the-arm interferometer

The fixed antennas are small in diameter, while there is thermal noise in the receiving routes #1 and #2, thus producing poor S/N ratios. After correlation processing, however, noise is reduced because the noise from the two receiving routes is mutually independent. The S/N ratio then improves significantly, allowing detection and measurement of weak satellite signals. The use of correlation processing also makes it possible to measure non-modulated beacons and modulated communication signals without discrimination.

Figure 3 shows the rotary arm with mirrors, and the fixed antennas. There are two sets of fixed antennas: the upper ones for the Ku band (11-12 GHz), and the lower ones for the C band (3-4 GHz). To select a receiving frequency band, mirrors  $M_3$  and  $M_4$  (Fig. 4) are tilted so that the microwave beams are directed to the right antennas.

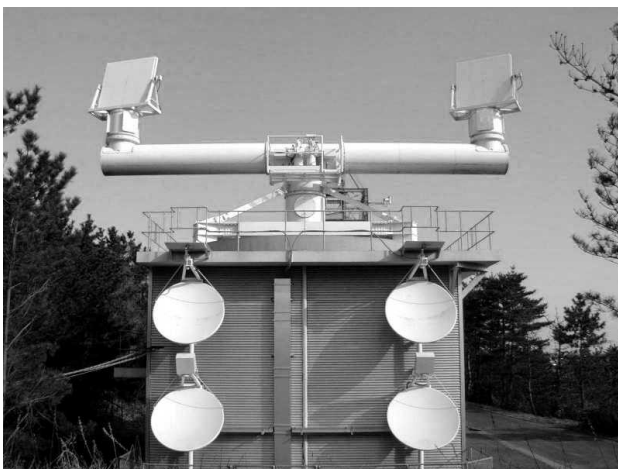


Fig. 3 Arm with mirrors, and fixed antennas



Fig. 4 Mirrors  $M_3$  and  $M_4$

### 3. R-MODE OPERATION

We use the following procedure to operate our interferometer. Choose a target geosynchronous satellite, and set the receiving beams to the azimuth and elevation  $(\alpha_0, \epsilon_0)$  at which the satellite should nominally exist. Set the receiving frequency so that a signal enters the phase-measuring processor. Advance the arm orientation angle in small steps to  $\theta_1, \theta_2, \dots, \theta_N$  over one revolution, and at each step measure the phase:  $\phi_i, i=1, 2, \dots, N$ . One arm revolution with measurements takes about 20 minutes using 15-degree steps. We call this the “R mode” (R for rotary).

As the arm angle advances, the measured phase changes, and when the phase exceeds  $2\pi$  it jumps back to zero. Examples are shown in Fig. 5, with “O”-marked data making jumps. We detect the jumps and reconnect them, so as to reconstruct a continuous curve over one revolution of the arm, as shown by the “O” and “+” marks in Fig. 5. The undulating shape of this curve determines the satellite’s direction. Denote the reconnected phase data as  $\hat{\phi}_i, i=1, 2, \dots, N$ .

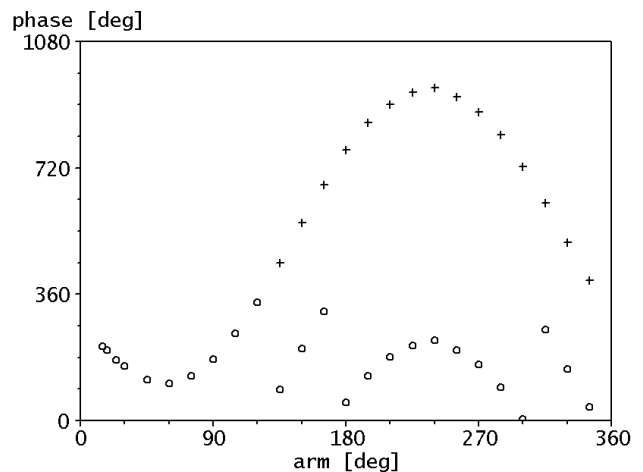


Fig. 5 Reconnecting the R-mode phase data

Meanwhile we prepare a theoretical model of the interferometer. For a satellite assumed at azimuth  $\alpha$  and elevation  $\varepsilon$ , set up a “path-delay function,” referring to the interferometer geometry as:

$$f(\alpha, \varepsilon, \theta) = [\text{Satellite-M}_2\text{-M}_4 \text{ path length}] \\ - [\text{Satellite-M}_1\text{-M}_3 \text{ path length}]$$

where  $\theta$  is the arm angle. The theoretical phase model is then defined as

$$\Phi_i(\alpha, \varepsilon, C) = (2\pi/\lambda)f(\alpha, \varepsilon, \theta_i) + C,$$

where  $\lambda$  is the receiving wavelength. By fitting the model  $\Phi_i(\alpha, \varepsilon, C)$  to the data  $\phi_i$ , we can determine the parameters  $\alpha$ ,  $\varepsilon$ , and  $C$ . The  $\alpha$  and  $\varepsilon$ , satellite azimuth and elevation are determined without ambiguity, as in the middle of the R-mode operation time. The constant  $C$  has two parts:  $C = C_p + 2n\pi$ , where  $C_p$  is a fraction of a cycle. This  $C_p$  indicates the phase-bias arising from the relative delay for the mirror-antenna paths of  $M_3\text{-A}_1$  and  $M_4\text{-A}_2$ . The  $2n\pi$  indicates phase ambiguity and has no physical meaning. Because the term  $C$  exists, the path-delay function need not consider the paths  $M_3\text{-A}_1$  and  $M_4\text{-A}_2$ .

The residual of the fitting,  $\tilde{\phi}_i - \Phi_i$ , indicates the performance of the interferometer. An example is shown in Fig. 6, where the RMS residual is 8.9 degrees. This corresponds to a length of 0.6 mm; that is, mechanical instability was as little as 0.6 mm when the arm and mirrors moved.

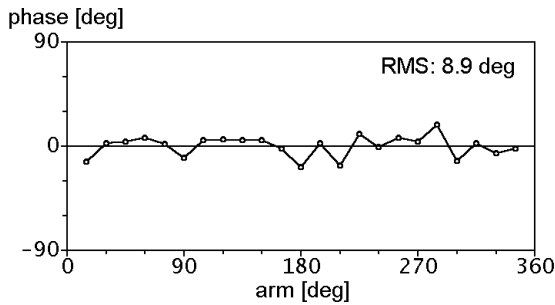


Fig. 6 Model-fitting residual, Ku band

The theoretical model is also used in phase reconnection. Consider a data set:  $\phi_i - \Phi_i(\alpha_0, \varepsilon_0, 0)$ ,  $i=1, \dots, N$ , as an “off-nominal” phase. Reconnection is easier for the off-nominal phase because it changes slowly with the arm angle. The data shown in Fig. 5 are off-nominal phases.

#### 4. X-MODE OPERATION

To find the latitude and longitude of a satellite’s motion, we need its orbit estimation. Theoretically speaking, we can repeat the R-mode operations to acquire azimuth and elevation data in succession for orbit estimation. However, because this forces excessive running of the rotary arm, we use a different mode.

First, we operate the R mode once to determine  $\alpha$ ,  $\varepsilon$ , and  $C_p$ . Next, we use only two arm angles, typically  $\theta_A = 135$

degrees and  $\theta_B = 225$  degrees. Phase data are measured at  $\theta_A$ , and after an interval, at  $\theta_B$ , again at  $\theta_A$ , and so on at regular intervals. The baseline cycles back and forth between the two positions, as illustrated in Fig. 7, which we term “X mode.”

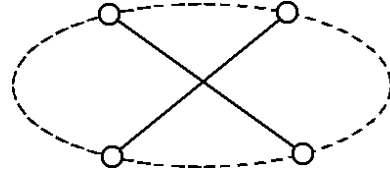


Fig. 7 X-mode operation

The phase data thus measured are processed one by one by filtering. The filter includes a model of satellite dynamics that considers the Earth’s asymmetric gravity and the sun/moon gravity. Solar-radiation pressure is not considered explicitly but is treated as noises in the satellite’s velocity. When phase-measurement data is acquired, we correct it for the bias  $C_p$  that has been determined in the R mode. Then, using the theoretical-phase model, we set the O–C. This O–C is normalized into the range of  $[-\pi, \pi]$  by adding or subtracting  $2n\pi$ . We then update the satellite’s state of motion, thus establishing its present latitude and longitude. The cycle of measurement data acquisition should not occur over too long a period because otherwise the O–C normalized into  $[-\pi, \pi]$  may be incorrect and the filtering falls into a wrong state. A few hours is an adequate cycling period for a satellite under normal station keeping. In addition, the initial orbital state must be sufficiently accurate and is prepared as follows. Assume a circular orbit with a nominal 42165-km radius. Adjust its inclination and mean anomaly so that the satellite azimuth/elevation agrees with the  $\alpha$  and  $\varepsilon$  that has been determined in the R mode. That is, the R mode operates as a starter for the X mode.

An example of X-mode monitoring is shown in Fig. 8. The arm-motion cycle period is one hour. The filter converges in half a day. After convergence, stable estimation continues. Orbital corrections, one NS and one EW, are seen in this example. The latitude and longitude of satellite motions can thus be monitored in real time.

If there are two satellites operating in the same frequency band, they can be monitored simultaneously, as shown in Fig. 9. In this example, the satellites are using one orbital position together. Here, we calculate the relative position of the satellites. This produces better precision because any error common for two satellites is cancelled out [2]. Plotting the relative motion in three dimensions (Fig. 10 on last page is an example) clarifies how the satellites are maintaining a distance for safety. Precise monitoring of the satellite orbit thus becomes possible.

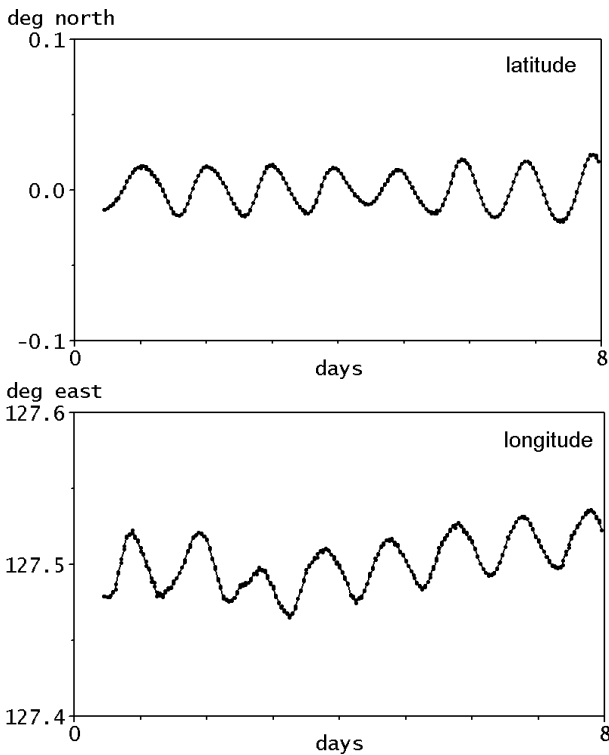


Fig. 8 X mode, in Ku band

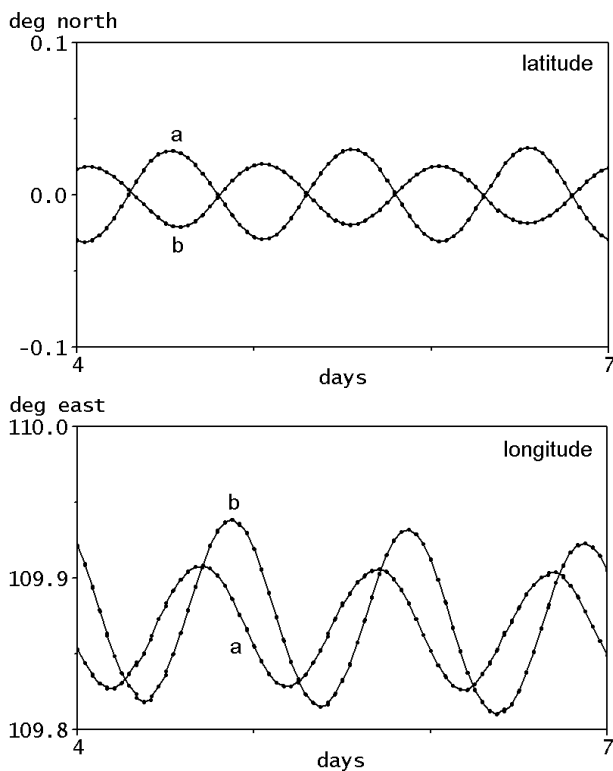


Fig. 9 X mode for two satellites (a/b), in Ku band

## 5. L-MODE OPERATION

If we regard satellite orbital positions as valuable “resources”, then orbital longitudes are of particular importance. If we are to evaluate how this resource is being consumed, we need to monitor satellite longitudes over the long term, and this is done using the following “L mode” (L for longitude).

In this mode, the rotary arm is fixed at a chosen angle. This choice must satisfy several conditions. In Fig. 11, an interferometer with baseline  $B$  (size is exaggerated) is placed at a monitoring station,  $M$ . The nominal position of our target satellite is  $S$ . Consider a line  $SD$  such that  $SD$  is orthogonal to the line-of-sight  $MS$ , and that  $SD$  and  $B$  lie in the same plane. When the satellite undergoes a displacement, its component along the  $SD$  is detected by the interferometer, i.e., the  $SD$  is the “detection line” of the interferometer. We want this  $SD$  to lie on the equatorial plane. This occurs when baseline  $B$  is at a chosen orientation, and at this orientation the arm angle is fixed. (Note that the arm angle depends on the relative geometry of  $M$  and  $S$ .) When our interferometer is set up thus in L mode, it only detects the satellite’s motion in the equatorial plane. Finally, consider a line  $ST$  that is tangent to the orbit at  $S$ . The satellite longitude is measured along  $ST$ , while the interferometer measures the satellite position along  $SD$ . Lines  $SD$  and  $ST$  form an angle depending on the  $M$ - $S$  geometry, and this angle never exceeds 8.7 degrees.

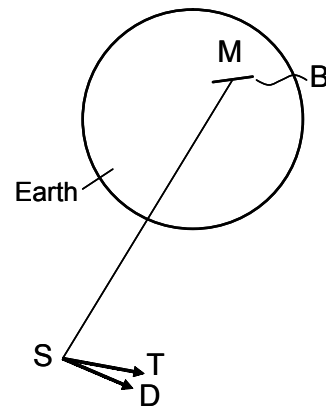


Fig. 11 L-mode geometry

We now have a problem to solve: Observed a satellite’s motion along  $SD$ , estimate its motion component along  $ST$ . This is solved as follows. First, as in the case of X mode, we operate the starter R-mode to determine  $\alpha$ ,  $\epsilon$ , and  $C_p$ . Next, the arm is fixed at the L-mode angle, and phase data are measured at regular intervals. Each time measurement data is acquired, we do the same filtering as in X mode, and thus determine the satellite’s present longitude. The only difference here is that the dynamics model assumes a fictitious satellite moving in the equatorial plane. That is, the satellite’s out-of-plane position and velocity are fixed to zero. The filtering must therefore start from a zero-inclination initial orbit.

An example of L-mode monitoring is shown in Fig. 12. Here, two satellites were found, one in the Ku band and the other in the C band, operating in proximity. Phase data were acquired every hour for Ku and C, with alternate switching of receiving bands. The starter R-mode was run for both bands. Monitoring continued for two cycles of EW station keeping. Obviously, station keeping was being coordinated between the satellites, allowing the two satellites to operate in a narrow longitude band. These satellites belong to different nations, and are using the orbital resource with good efficiency through coordination. We can thus use the L-mode to monitor the state of orbital resource consumption.

Here, we suggest a simple version of our L-mode interferometer for satellite operators. Suppose we are operating our satellite at a location S in Fig. 11. As the M-and-S geometry is fixed, the mirrors are placed in fixed positions. Since our satellite's beacon is known, a simple phase meter replaces the correlation processor. The interferometer thus requires only simple hardware. The starter information will be provided by the station-keeping orbit determination. Real-time longitudes output from this interferometer will be important if there is another satellite from a different agency or nation operating in proximity with ours, like in the case of Fig. 12. If our satellite uses electric propulsion, its orbit will show some unpredictable behavior. Real-time longitudes are then important for its station keeping. Our L-mode interferometry will thus find application in satellite operations of the future.

## 6. ERROR CALIBRATION

We need to know the geometry of the interferometer accurately to set up the path-delay function. However, surveying the arm and mirrors using theodolites and measures may introduce errors. The error parameters that affect satellite tracking accuracy have been identified as:

- Error in arm length ( $\delta L$ )
- Bias error in arm angle ( $\delta\theta$ )
- Tilt of arm-rotating plane from horizontal: north-up ( $X$ ) and east-up ( $Y$ )

We calibrate these error parameters as follows. Choose  $K$  satellites with equal spacing along the visible orbital arc. For each satellite, perform the R mode and reconnect the phases. At the same time, determine satellite # $j$ 's azimuth and elevation ( $\alpha_j, \epsilon_j$ ),  $j=1..K$ , using optical observation [3] and assume them to be true. Meanwhile, rewrite the path-delay function so that it has four additional arguments denoting the error parameters. The theoretical phase model for satellite # $j$  then becomes

$$\Phi_{j,i} = (2\pi/\lambda_j) f(\alpha_j, \epsilon_j, \theta_j, \delta L, \delta\theta, X, Y) + C_j.$$

We fit this model to the above-obtained reconnected data, with  $\alpha_j$  and  $\epsilon_j$  assumed as known. The error parameters

are unknown and common for all satellites. The fitting is therefore processed for all data combined, and this leads to the solution of  $\delta L$ ,  $\delta\theta$ ,  $X$ , and  $Y$ . Experiments have shown that five reference satellites ( $K=5$ ) are perfect. The errors determined so far are:  $\delta L = 2.3$  mm,  $\delta\theta = -0.004$  degrees,  $X = 1.3$  mm,  $Y = -0.7$  mm. This result is reasonable if we consider the accuracy of the survey we have used. The path-delay function with these parameters fixed is then used in the R/X/L-mode operation. This procedure of error calibration enables us to maintain an accuracy in the order of milli-degrees for satellite direction measurements.

Note that the length of the arm changes with temperature. The air temperature fluctuates by over 30 degrees or more in a year, causing the length to vary by as much as 4 mm. For this reason, arm-temperature data are collected along with phase data to correct the arm length. The design of our interferometer enables us to easily model the thermal effect as a one-dimensional change in the arm length. If we used a large parabolic antenna, thermally caused distortions would be complicated when the sunlight irradiated from changing directions, and these errors would be impossible to correct using a model.

## 7. CONCLUSION

As a result of using a rotary baseline, our interferometer is capable of

- determining satellite azimuth/elevation without ambiguity
- estimating satellite latitude/longitude motions in real time
- estimating satellite longitude motions over the long term

with an accuracy better than 0.01 degrees. These capabilities apply to any visible satellite, even with no prior knowledge of the satellite. Using this interferometer we can survey the state of orbital congestion and evaluate orbital resource consumption. Satellite operators who are anxious about orbits could use a fixed L-mode interferometer for real-time monitoring of satellite longitudes.

## REFERENCES

1. *Handbook - Spectrum Monitoring, Edition 2002*, ITU.
2. Kawase and Sawada: Interferometric Tracking for Close Geosynchronous Satellites, 12th International Symposium on Space Flight Dynamics, Darmstadt, June 1997.
3. Umehara: Ground-based optical scan and parallel orbit determination of near-geosynchronous objects, 21st Communications Satellite Systems Conference, Yokohama, April 2003.

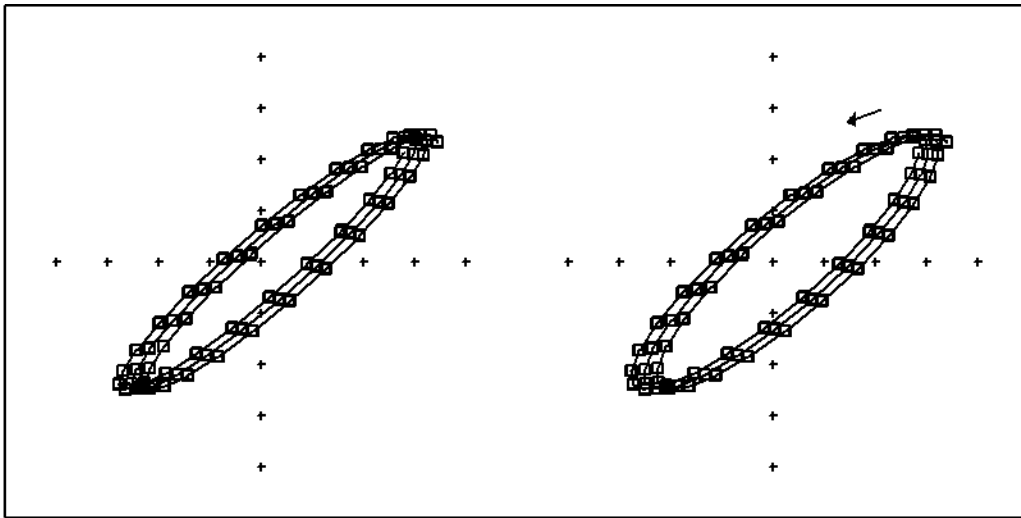


Fig. 10 Relative satellite motion from Fig. 9, b minus a, in stereograph.  
 One "+" division is 0.02 degrees of latitude/longitude, north: up, east: right

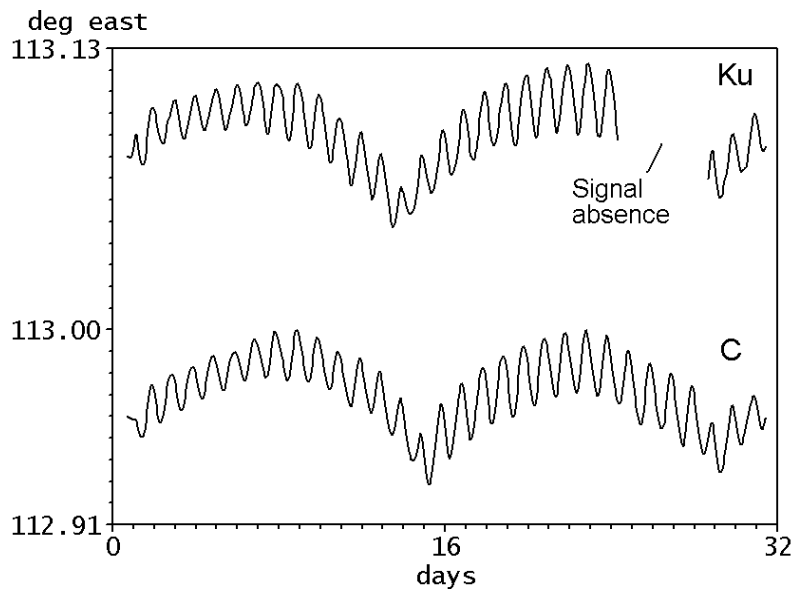


Fig. 12 Long-term longitudes by L mode